IEEE Access
Multidisciplinary | Rapid Review | Open Access Journal

Received April 19, 2019, accepted May 5, 2019, date of publication May 29, 2019, date of current version June 7, 2019.

Digital Object Identifier 10.1109/ACCESS.2019.2918726

A Task-Driven Updated Discrete Graph Assisted Minimum Delivery Delay Routing for Remote Sensing Disruption-Tolerant Networks

PENG YUAN, ZHIHUA YANG, YE WANG, SHUSHI GU, AND QINYU ZHANG
College of Electronic and Communication Engineering, Harbin Institute of Technology (Shenzhen), Shenzhen 518000, China

Corresponding author: Qinyu Zhang (zqy@hit.edu.cn)

This work was supported in part by the National Natural Sciences Foundation of China under Grant 61831008, Grant 61701136, Grant 61571156, and Grant 61525103, in part by the Guangdong Science and Technology Planning Project under Grant 2018B030322004, in part by the Natural Science Foundation of Guangdong Province under Grant 2016A030313661, and in part by the Shenzhen Basic Research Program under Grant ZDSYS201707280903305.

ABSTRACT Benefiting from the extensive coverage, remote sensing satellites have been playing important roles in surveillance for regions on the earth surface. In order to accommodate with intermittent connected and partitioned characteristics of satellite topology, disruption-tolerant network (DTN) develops a feasible solution for networking among such satellites. However, utilized widely and frequently in the future, numerous image covering hundreds of spectral bands and kilometers width is supposed to be delivered simultaneously. Due to the timeliness constrain, efficient routing design with minimum delivery delay for bulk and concurrent image data has become the bottleneck of remote sensing application. Considering data transmission initiated as different tasks, therefore, the Task-driven Updated Discrete Graph (TUDG) is designed to depict the topology evolution, with task data and edge capacity model for BP/LTP incorporated Remote Sensing DTN Network (RS-DTNet). In particular, the multitask-based delivery delay analytical framework is proposed based on the TUDG graph model, by solving a mixed integer Max-Min optimization problem. The Multi-Task Minimum Delay Routing (MTMDR) is designed with the delay-optimal flow distribution, dispatching appropriate bundle data to edges in the TUDG. This flow-based routing avoids the path selection procedure, which may degenerate the delivery delay performance. Through numerical simulation based on the representative RS-DTNet scene, the proposed MTMDR routing strategy shows to advantage on delivery delay, compared with typical path-based routing.

INDEX TERMS Delivery delay, disruption-tolerant network, min-max optimization, remote sensing.

I. INTRODUCTION

To meet with the increasing demands for geological and weather information, remote sensing satellites, interconnected as constellation networks, have been playing important roles in surveillance for resource, environment, disaster and so on, benefiting from the extensive coverage [1], [11]. Equipped with different sensors onboard, numerous types of image files are generated, and delivered towards the ground centers for further processing.

Generally speaking, the remote sensing images detail the Region of Interest (RoI) on the earth surface, with high distance resolution, even achieving sub-meter level. Meanwhile, for the sake of multi-categories and wide-area surveillance, such images cover hundreds of spectral bands and kilometers width. Correspondingly, the remote sensing image files are usually with large quantity of data [5]. The swing capacity of satellites improves the temporal resolution [6] for imaging, and enables flexible surveillance, however, makes the size of task data more difficult to be estimated.

Moreover, utilized widely and frequently in the future, numerous remote sensing images are supposed to be generated and transferred to the ground centers simultaneously. On the other side, data transmission is limited by the long distance and confined contacts between remote sensing satellites and ground centers. The intermittent connected and partitioned characteristics of satellite topology further deteriorate the remote sensing images backhaul [2]. Thus, considering

The associate editor coordinating the review of this manuscript and approving it for publication was Mohammad Tariqul Islam.

such bulk and concurrent image data, efficient routing design has become the bottleneck of remote sensing application.

In order to evaluate the performance for the routing design, several metrics are proposed, including the delivery delay [3]. Typically, delivery delay is crucial for delay-sensitive tasks, and related to other metrics such throughput and delay jitter. Even for the delay-nonsensitive tasks, data backhaul befits from the decrease of delivery delay, which can alleviates the resource demand, such as storage onboard [7]. The conventional definition of delivery delay focus on the single packet, which can be attributed as searching for delay-optimal routing path. Nonetheless, considering data transmission initiated as different tasks, task-based delivery delay (TDD) is more suitable to evaluate the temporal requirement for the given image data size in remote sensing networks. In our previous work [28], the minimum TDD for single task is designed. However, minimum TDD and corresponding data routing path for multi tasks are constrained by the concurrent bulk data and varying network topology, which deserves more research.

Therefore, in this paper, a multi-task based delivery delay analytical framework for remote sensing Disruption-Tolerant Networks is proposed. Compared with conventional path-based methods, the proposed framework allocates image data from different task to corresponding contacts with optimal flow. The Task-driven Updated Discrete Graph (TUDG) graph is designed, taking the image data model into consideration. In particular, TUDG graph achieves compromise between model accuracy and complexity, which is appropriate for RS-DTNet. Based on the TUDG graph, the data transmission constrains can be converted into weight of vertexes and edges. The minimum TDD for multi-tasks can be calculated through solving optimization problem, accompanied by the corresponding Multi Task Minimum Delay Routing (MTMDR). Compared with previous works, this paper has the following contributions: (1) The Task-based Updated Discrete Graph (TUDG) is proposed for the remote sensing satellites with swing capacity and multi-spectrum, to depict the topology evolution in RS-DTNet. (2) Based on the TUDG graph model, multi-task based delivery delay analytical framework is built, which can be utilized to analyze the delay-related performance. (3) The MTMDR routing strategy is designed with minimum delivery delay. For the numerical simulations, the proposed routing algorithm MTMDR and typical path-based routing strategy is evaluated, by a joint simulation environment. Through the extensively experimental results, the MTMDR algorithm shows significant performance improvements with respects to the delivery delay.

The remainder of the paper is organized as follows. Section II details the related works of RS-DTNet, where different graph models are summarized. Section III introduces the system model and TUDG graph model with the task data model for RS-DTNet. The mathematical model of edge capacity is presented, in considering of the transmission procedure with BP/LTP architecture. Section IV describes minimum delvery delay problem for multi-tasks. The MTMDR routing algorithm is proposed, through solving an *Max-Min* optimization problem. Then, the performance discussions are shown in section V. Finally, we draw the conclusions in section VI.

II. RELATED WORKS

A. REMOTE SENSING DISRUPTION TOLERANT NETWORK

Due to the rotation of earth and revolution of satellites, nodes in Remote Sensing Network (RSNet) are intermittent connected. Even if these two nodes are visible to each other, the huge distance leads to long prorogation delay and high data error rate, which is quite different from the contacts in terrestrial networks [12]. Furthermore, task imaging time and size, depending on the relative position between remote sensing satellites and RoI, change over time. Thus, image data for different region suffers different network topology evolution during transmission from the source to destination. To cope with such challenge in RSNet caused by time-varying and divisional topology, Remote Sensing Disruption-Tolerant Network (RS-DTNet) is proposed [14], with specific-designed store-forward and retransmission mechanism. In [15], large image file transfer experiments for the remote sensing satellites were performed, with Bundle Protocol (BP) overlaying different sub-networks. Particularly, the performance of BP and convergence layer adapter (CLA) protocols is evaluated in [16], which highlights the advantage of Licklider Transmission Protocol (LTP) for space communication environment with long link delay and lengthy link disruptions. In [17], the analytical model of transmission performance with BP is proposed in a heterogeneous space networking system, and the effect of link disruptions is evaluated. In summary, the research for RS-DTNet focuses on influence of the challenging environment based on the simulation test-bed infrastructure, without complete theoretical analysis.

B. GRAPH MODEL FOR RS-DTNET

Based on the architecture of RS-DTNet, different kinds of graph model are designed to describe the network characteristics. The vital issue for the graph design is definitions of vertexes and edges, and corresponding weights. Based on the different structure, these models can be grouped into two categories: the aggregated and extended graph. To avoid ambiguity, nominal ''node'' and ''contact'' are used for the RS-DTNet, ''vertex'' and ''edge'' are applied to the graph model, on the contrary.

Basically, the aggregated graph model duplicates network topology, and contains only one copy of each node in RS-DTNet. The representative aggregated graph model is Storage Time Aggregated Graph (STAG) $\mathcal{GA} = \langle EA, VA \rangle$ [18]. In order to capture topology changes, the time span considered for the tasks is divided into numerous small successive intervals. The weight of edges are defined with capacity time series. Furthermore, the vertexes are labeled with bidirectional storage transfer series, which can model the data storage in intermediate nodes. Both capacity and storage

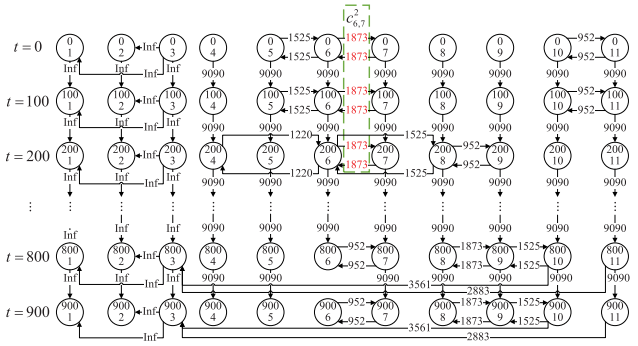

FIGURE 1. Time expanded graph model.

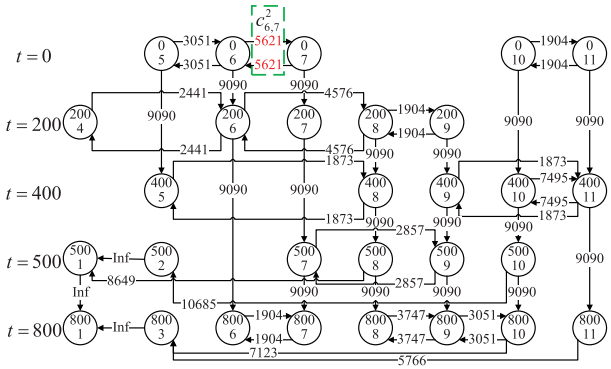

FIGURE 2. Event-driven graph model.

series are attached to the time intervals mentioned above. However, due to the intermittent connectivity for the contacts in RS-DTNet, routing for image data in the aggregated graph model requires special design, based on the auxiliary information such as weight series of vertexes and edges.

On the contrary, the extended graph model expands the network topology in the time dimension, and multiple replicas of nodes coexist and are connected with additional edges representing the storage process. Similarly, due to the topology evolution can be regarded as a serial of snapshots with fixed time discretization interval τ_t, Time Expanded Graph (TEG) $\mathcal{GT} = \{GT_{l_t} | 1 \leq l_t \leq L_t\}$ is designed [19], shown as Fig. 1 with network topology defined in Table. 2. Every sub-graph $GT_{l_t} = \langle ET_{l_t}, VT_{l_t} \rangle$ represents the l_t-th snapshot of RS-DTNet. There are temporal and spatial edge in TEG. Specifically, the temporal edge connects the same node in the adjacent sub-graph GT_{l_t} and GT_{l_t+1}, labelled with the storage size in the corresponding node. And spatial edge represents the discrete contact in sub-graph GT_{l_t}, weighted with discrete contact capacity. It can be proven that τ_t should take small enough value, in order to capture subtle topology change. Thus, the tradeoff between graph complexity and accuracy should be taken into consideration. Besides, time instance at the intermediate nodes for data transmission fastens to integral multiple of discretization interval τ_t, introducing extra quantization error.

Considering the difficulty for setting appropriate value of τ_t, the Event-Driven Graph (EDG) $\mathcal{GE} = \{GE_{l_e} | 1 \leq l_e \leq L_e\}$ is proposed [20], characterizing as elastic discretization interval $\tau_e^{i,j}$ between the j-th and i-th layer, $1 \leq i \leq j \leq L_e$. An example of EDG is shown as Fig. 2 with network topology defined in Table. 2. It is assumed that $j = i$ when $\tau_e^{i,j} = 0$, which means contacts with the same begin time are in the same layer. The contact in RS-DTNet converts into two vertexes, labelled with node and time instance, respectively. Similarly, edges in EDG are divided into temporal and spatial ones, referring to the TEG. Apparently, the value of layers in EDG equals number of unique time instance for contact begin time. Thus, the size of EDG is much more smaller than TEG, without handling the intractable value of τ_t. However, only with regard to topology change whenever the contact begins, the holistic evolution is still difficult to be characterized accurately, especially for the overlapping long contacts.

C. TASK DELIVERY DELAY

Through the contacts with long geometrical distance and limited transmission rate, data transmission in RS-DTNet is subjected to significant propagation and transmission delay. Furthermore, intermittent contact connectivity and partitioned network topology result in the difficulty for end-to-end communication, which implies redundant delay. Though asynchronous data transmission mechanism is adopted in RS-DTNet, delivery delay for the given task is still an important performance evaluation parameter. In [21], the basic transmission procedure of BP is illustrate, with the excepted delivery is estimated. In [17], bundle delivery time model for single and multiple contacts are proposed. Particularly, the influence of the space contact disruption is analyzed. Several end-to-end delivery delay analytical models based on tandem queuing theory [22] and Markov chain [23] are proposed, which focus on single packet. Moreover, the Contact Graph Routing (CGR) and representative enhancements is surveyed in [24], which can find the routing path with minimum end-to-end delivery delay with distributed scheme. Typically, CGR utilizes the contact plan, which records the scheduled, anticipated topology changes in time-order, and finds the earliest transmission opportunity for data packet with the Dijkstra searches in an abstract contact graph. However, the importance of the task size on delivery delay is scarce acknowledged, associated with the path capacity. In [25], the influence of traffic and time-varying topology parameters on end-to-end deliver delay is analyzed. The Continuous Time-varying Graph based Routing (CTGR) is proposed, with the graph classified as aggregated model. The performance for different data size is evaluated. Nonetheless, the CTGR routing is based on path with minimum delivery delay from the source to the destination, where data size is allocated according to the path capacity. The delay-optimal path may change once data is transferred, in consideration of the time occupied by data transmission. Thus, path-based routing is not suitable for data transmission design with minimum TDD. Furthermore, the influence for delivery delay

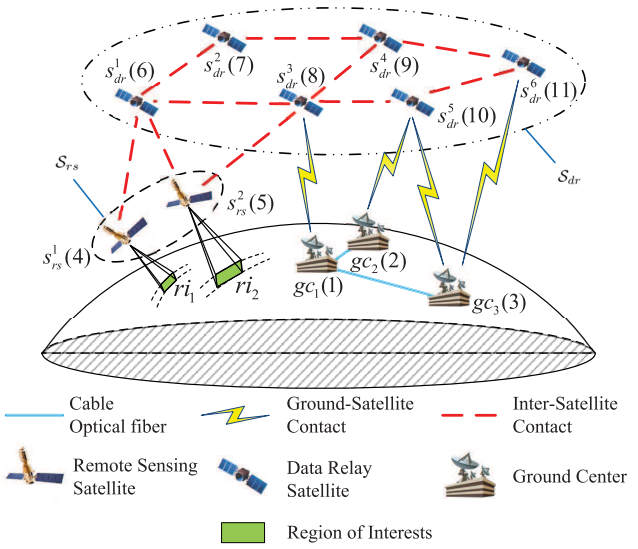

FIGURE 3. Remote sensing network model.

with multi tasks is has been seldom studied, which may occur frequently in the future.

III. TASK-DRIVEN UPDATED DISCRETE GRAPH

A. SYSTEM MODEL

Generally speaking, the typical RS-DTNet comprises satellite set $\mathcal{S} = \{s_m | 1 \le m \le M\}$ and ground center set $\mathcal{GC} = \{gc_l | 1 \le l \le L\}$ [13]. In consider of the different equipments onboard, $\mathcal{S}$ can be categorized into remote sensing satellite set $\mathcal{S}_{rs} = \{s^{m_1}_{rs} | 1 \le m_1 \le M_1\}$ and data relay satellite set $\mathcal{S}_{dr} = \{s^{m_2}_{dr} | 1 \le m_2 \le M_2\}$, further expressed as $\mathcal{S} = \mathcal{S}_{rs} \cup \mathcal{S}_{dr}$, $M = M_1 + M_2$. For the convenience of illustration, all nodes in RS-DTNet, represented as $\mathcal{N} = \{n_i | 1 \le i \le N, N = L + M\}$, are numbered from 1 to N, in the order of $\{\mathcal{GC}, \mathcal{S}_{rs}, \mathcal{S}_{dr}\}$. An example of such RS-DTNet is demonstrated in Fig. 3, with corresponding serial number in the brackets, respectively.

The data flow in remote sensing networks includes forward (from ground center to satellite) and reverse (from satellite to ground center) directions [8]. Initially, the RoI set $\mathcal{RI} = \{ri_j | 1 \le j \le J\}$ are predefined by ground centers. Taking advantage of priori knowledge of $\mathcal{S}_{rs}$ orbit parameters and $\mathcal{RI}$ location coordinates, the mutual visibility and illumination condition can be estimated according to geometry [4]. Thus, image acquisition tasks plan are scheduled at ground center $\mathcal{GC}$ and uploaded to competent satellite $s^{m_1}_{rs}$, with assigned task ri_j.

Utilizing the sensor equipments such as Operational Land Imager (OLI) and Thermal Infrared Sensor (TIRS) [9], $s^{m_1}_{rs}$ generates multi spectral bands image files for ri_j, whose format is introduced in [10]. After data acquisition, the image files are downloaded back to the ground center gc_l through a serial of contacts, and then gathered to the appointed place (such as gc_1 in Fig. 3). In the similar way, contact between two node at any time can also be calculated aforehand, as well as the distance and direction. With the specifications of

TABLE 1. Contact list.

k	n^k_f	n^k_t	T^k_b/s	T^k_e/s	T^k_p/s	P^k_b	R^k/Mbps
1	5	6	0	200	0.01	10^{-5}	50
2	6	7	0	300	0.01	10^{-6}	50
3	10	11	0	200	0.02	10^{-5}	50
4	4	6	200	400	0.02	10^{-6}	50
5	6	8	200	500	0.01	10^{-5}	50
6	8	9	200	400	0.02	10^{-5}	50
7	5	8	400	500	0.01	10^{-6}	50
8	9	11	400	500	0.01	10^{-6}	50
9	10	11	400	800	0.01	10^{-6}	50
10	7	9	500	800	0.02	10^{-5}	50
11	8	1	500	800	0.005	10^{-5}	100
12	10	2	500	800	0.005	10^{-6}	100
13	6	7	800	1000	0.02	10^{-5}	50
14	8	9	800	1000	0.01	10^{-6}	50
15	9	10	800	1000	0.01	10^{-5}	50
16	10	3	800	1000	0.005	10^{-6}	100
17	11	3	800	1000	0.005	10^{-5}	100

TABLE 2. Comparison for different graph models.

Evaluation Metrics		TEG	UDG	EDG	STAG
Vertexes	Max	476	103	31	17
	Mean	204	57.9	25.3	16.7
	Min	34	33	21	16
Edges	Max	1149	392	66	29
	Mean	493.3	200.4	57.4	25.8
	Min	80	100	50	22

communication equipments and geometric positions, the contact list $\mathcal{C} = \{c^k_{f,t} | 1 \le k \le K\}$ is established, whose element $c^k_{f,t}$ represents the k-th contact in the set. Typically, $c^k_{f,t}$ is labelled with seven elements, i.e., contact from node n^k_f, to node n^k_t, begin time T^k_b, end time T^k_e, prorogation delay T^k_p, bit error rate P^k_b and transmission rate R^k, shown in Table. 2. Furthermore, according to different type of nodes, $\mathcal{C}$ can be divided into Inter-Satellite Contact (ISC) set $\mathcal{C}_{is} = \{c^{k_1}_{f,t} | 1 \le k_1 \le K_1\}$ and Ground-Satellite Contact (GSC) set $\mathcal{C}_{gs} = \{c^{k_2}_{f,t} | 1 \le k_2 \le K_2\}$, $\mathcal{C} = \mathcal{C}_{is} \cup \mathcal{C}_{gs}$, $K = K_1 + K_2$. It is notable that $c^k_{f,t}$ is GSC if $n^k_t \in \mathcal{GC}$, otherwise $c^k_{f,t}$ is ISC. Besides, every ground center in $\mathcal{GC}$ is equipped with infinite storage, and connected with cable or optical fiber, which can be regarded with infinite data transmission capacity.

B. BASIC RULES

Basic on the design criteria for the TEG and EDG, the Task-driven Updated Discrete Graph (TUDG) $\mathcal{GU} = \{GU_{l_u} | 1 \le l_u \le L_u\}$ is proposed, with elastic discretization interval τ_u.

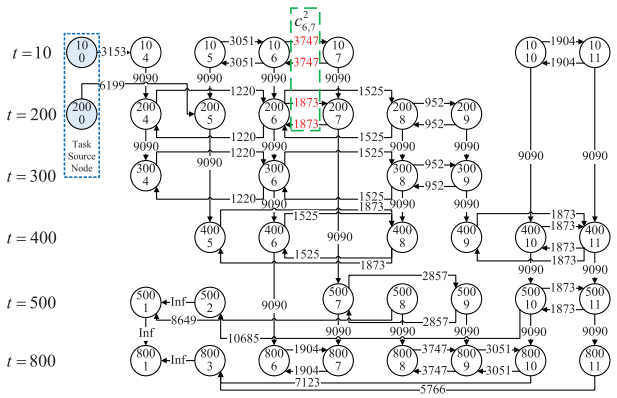

FIGURE 4. Task-driven updated discrete graph.

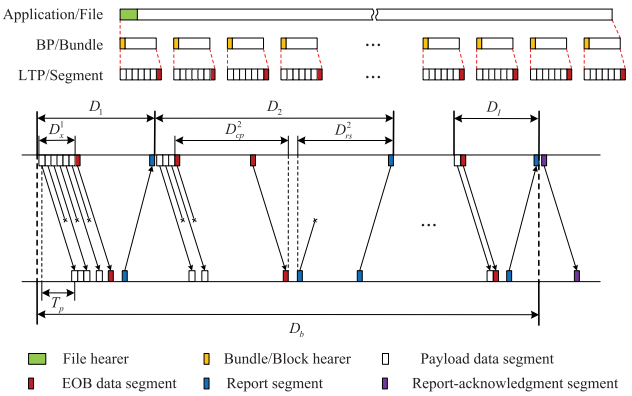

FIGURE 5. Transmission procedure model.

TABLE 3. Protocols data parameter list.

Name	Description	Value
H_b	Size of bundle header/Kb	0.1
N_s	Nof segments in bundle	1000
H_s	Size of segment header/Kb	0.1
M_s	Size of segment payload/Kb	1
M_r	Size of report segment/Kb	0.1

The definition and label of vertexes and edges are similar with EDG. And $eu^{ii}_{l_u,l_u+1}$ and $eu^{ij}_{l_u,l_u}$ are defined as the temporal edge and spatial edge, respectively. However, different from the EDG model, the UDG graph is updated whenever the network topology changes, including both T^k_b and T^k_e, $1 \le k \le K$. For simplify, time set $\mathcal{T}_{tc} = \{t^{k_t}_{tc} | 1 \le k_t \le K_t\}$ is used to record the time instance when topology changes. $\mathcal{T}^{k_t}_{tc}$ includes unique contact begin time T^k_b and end time T^k_e, restored in chronological order. And every contact duration is divided into several segmentations, according to the time set $\mathcal{T}^{k_t}_{tc}$, in order to handle the long and overlapped contacts. Befitting from the elastic discretization interval, the value of layers in UDG $L_u = |\mathcal{T}_{tc}| = K_t$. The remote sensing image acquisition task can be mapped as the source node in TUDG labelled with timestamp and node serial number, affiliates the traditional UDG graph with an edge labelled with task data size. The TUDG model for contact list in Table. 2 is shown as Fig. 4. Supposing that sl_k is the number of lays which contact $c^k_{f,t}$ spans, size of TUDG (evaluated by number of vertexes NV_u and edges NE_u) can be expressed as

$$\begin{aligned} NV_u &= \sum_{l_u=1}^{L_u} |VU_{l_u}| \le L_u \cdot N + J \\ NE_u &= \sum_{l_u=1}^{L_u} \sum_{i=1}^{N} \sum_{j=i}^{N} (|eu^{ii}_{l_u,l_u+1}| + |eu^{ij}_{l_u,l_u}|) \\ &\le \sum_{k=1}^{K} \alpha_k \cdot sl_k + L_u \cdot N + K_2 + J \end{aligned} \tag{1}$$

where

$$\alpha_k = \begin{cases} 1 & c^k_{f,t} \in \mathcal{C}_{gs} \\ 2 & c^k_{f,t} \in \mathcal{C}_{is} \end{cases}$$

Specifically, taking the second contact $c^2_{6,7}$ in $\mathcal{C}$ as illustration, different approaches for TEG, EDG and UDG are proposed, demonstrated in Fig. 1, 2 and 4. Because of $L_u \le L_t$, it can be concluded that the size of UDG is significantly less than TEG. Compared with EDG, the long contact $c^2_{6,7}$ is divided into two sub-contact, without change the topology evolution characteristic. In Table. (2), the number of nodes and edges of different graph models are compared, with the parameter setting described in Section V-A. The maximum, mean and minimum value are counted statistically for time instance varied from 0-80000s. Without loss of accuracy, the size of UDG is much less than TEG. Although EDG and STAG are more lightweight than UDG, modeling for the RS-DTNets is restricted by intrinsic defects mentioned in Section II-B.

C. EDGES CAPACITY MODEL

Coping with the challenging environment in RSNet, Bundle Protocol (BP) in Bundle Layer and Licklider Transmission Protocol (LTP) in Convergence Layer are adopted, which benefits from the pecific-designed store-forward and retransmission mechanism. The basic transmission procedure from the sender to receiver without disruption is demonstrated in Fig. 5. Initially, image file in the application layer is divided into several blocks, containing one or more bundle as the basic data unit in BP. Furthermore, data in bundle is subdivided into numerous segments. The primary segment structure comprise the image file payload, and the last one is marked as the End Of Block (EOB) segment, which acts as the Check Point (CP) for the block data. The CP segment informs the receiver to check the data integrity, and triggers a timer in the sender. Similarly, reception of the CP arouses the transmission of Report Segment (RS), with the scope of segments failed to be recovered, due to error or missing, accompanied by the timer in the receiver. For convenience of expression, the BP/LTP protocol data parameter list $\mathcal{D} = \langle H_b, N_s, H_s, M_s, M_r \rangle$, as demonstrated in Table. (3).

In order to ensure the reliability and integrality of data, selective negation retransmission mechanism is adopted repeatedly until the all segment are received successfully, with the report-acknowledgement segment. Thus, the single bundle data transmission procedure can be divided into several phases, whose delivery delay D_b from sender to receiver can be expressed as

$$D_b = \sum_{i=1}^{I} D_i = \sum_{i=1}^{I} (D_x^i + D_{cp}^i + D_{rs}^i) \tag{2}$$

where D_i is the bundle delay in the i-th phase, which includes payload segment transmission delay D_x^i, CP delay D_{cp}^i and RS delay D_{rs}^i. It is notable that *Phase-I* only comprises D_x^I, CP delay D_{cp}^I. However, due to the retransmission mechanism for payload, CP and RS segments, each component for D_i is uncertain, leading to D_b estimation with probability. Specifically, D_{cp}^i and D_{rs}^i can be expressed as

$$\begin{aligned} \Pr\left(D_{cp}^i = T_p + j \cdot (T_{cp}^x + T_{cp}^i)\right) &= p_{cp}^{j-1} \cdot (1 - p_{cp}) \\ \Pr\left(D_{rs}^i = T_p + j \cdot (T_{rs}^x + T_{rs}^i)\right) &= p_{rs}^{j-1} \cdot (1 - p_{rs}) \end{aligned} \tag{3}$$

where T_p is prorogation delay, T_{cp}^x/T_{rs}^x, p_{cp}/p_{rs} and T_{cp}^i/T_{rs}^i are the transmission delay, segment error rate and value set for timer of CP/RS segment, respectively.

On the other side, D_x^i is depends on data size DS^i and transmission rate R, which can be expressed as

$$D_x^i = DS^i/R \tag{4}$$

With the derivation from [21], the expectation and variance of D_b can be expressed as

$$\begin{aligned} E(D_b) &= E\Big(\sum_{i=1}^{I-1}(D_x^i + D_{cp}^i + D_{rs}^i)\Big) + E(D_x^I) + E(D_{cp}^I) \\ &= E(I-1) \cdot \Big(\frac{(1 - p_{cp}p_{rs}) \cdot (2T_p + T_{rs})}{(1 - p_{cp}) \cdot (1 - p_{rs})} + \frac{T_{cp}}{1 - p_{cp}}\Big) \\ &\quad + E(\sum_{i=1}^{I} D_x^i) + \frac{p_{rs}}{1 - p_{rs}} \cdot E(\sum_{i=1}^{I-1} D_x^i) + \frac{1 + p_{cp}}{1 - p_{cp}} \cdot T_p \\ &\quad + \frac{T_{cp}}{1 - p_{cp}} + \frac{p_{cp} \cdot T_{rs}}{1 - p_{cp}} \end{aligned} \tag{5}$$

$$\begin{aligned} V(D_b) &= V\Big(\sum_{i=1}^{I-1}(D_x^i + D_{cp}^i + D_{rs}^i) + V(D_x^I) + V(D_{cp}^I)\Big) \\ &= V\Big(\sum_{i=1}^{I}(D_x^i) + \sum_{i=1}^{I-1}(D_{rs}^i)\Big) \end{aligned} \tag{6}$$

It can be concluded that both $E(D_f)$ and $V(D_f)$ are finite. Generally speaking, due to the large size of the remote sensing image file, the number of encapsulated bundle are numerous. And delay D_b of different bundle can be regarded as *i.i.d.*. With the central-limit theory, the probability of sum delay bundles D_f^b follows the Gaussian distribution, when the number of $N_b \to \infty$, i.e.,

$$\Pr(D_f^b) \sim G\big(N_b \cdot E(D_f), N_b^2 \cdot V(D_f)\big) \tag{7}$$

Furthermore, with the analysis in [26], the protocols adopted has significant impact on the data transmission performance, especially for the space network with long propagation delay and intermittent connected topology. Particularly, due to the error-prone link and retransmission mechanism, data transmission capacity for the single contact is time varying, which cannot be evaluated in the intuitive link level, i.e., $R^k \cdot (T_e^k - T_b^k)$. Thus, in this paper, the contact capacity Cap_f^t is evaluated with packet level, which is defined as the number of bundles can be transferred successfully within limited contact duration, in considering of the network environment characteristics. Specifically, given the contact began at T_b^k and continued to T_e^k, Cap_f^t can be expressed as

$$D_f^{Cap_f^t} \le T_e^k - T_b^k \le D_f^{Cap_f^t+1} \tag{8}$$

From (7) and (8), Cap_f^t is related to contact duration, BP/LTP parameters, and channel environment. Befitting from the distribution of Cap_f^t concentrating around the exception, $E(Cap_f^t)$ is utilized as the edge capacity in UDG model, which can be expressed as

$$E(Cap_f^t) = \lceil (T_e^k - T_b^k)/E(D_b) \rceil \tag{9}$$

D. TASK DATE MODEL

With the pre-defined plan for the task $ri_j \in \mathcal{RI}$, image data is acquired by the satellite $s_{rs}^{m_1}$, utilizing the sensing equipments onboard. Benefiting from the stable geometry structure, 'push-broom' model sensor is widely adopted, with numerous pixels arranged in line for multi spectral bands. Operating with the movement of satellite, several banner images for every spectral band are acquired by those pixels, and then spliced as remote sensing image, during the working period of the sensing equipments. These images for different spectral band are encapsulated as file with numerous bundles, and then transferred back to the ground center, with data compression.

In order to get better imaging flexibility and shorter revisit interval, remote sensing satellites have the swinging ability. Thus, the region of imaging is not limited to the satellite sub-point track. However, the spatial resolution for the task changes, which has impact on the data size of image file, as shown in Fig. 6. Given $sr_{m_1}^b$ as the spatial resolution of sub-satellite point for the b-th spectral band in satellite $s_{rs}^{m_1}$, the resolution $sr_{m_1}^{b,j}$ with swinging θ_j for task ri_j can be expressed as

$$sr_{m_1}^{b,j} = sr_{m_1}^b \cdot h_{m_1}^j / h_{m_1} \tag{10}$$

where $h_{m_1}^j$ is the distance between satellite and the center of the banner image for ri_j. Setting R is the radius of Earth, $h_{m_1}^j$ can be expressed as

$$h_{m_1}^j = (h_{m_1} + R) \cdot \cos\theta_j - \sqrt{R^2 - (1 - \cos^2\theta_j)(h_{m_1} + R)^2}$$

Without loss of generality, the task imaging time T_t^j and duration T_d^j for task ri_j is decided according to task plan.

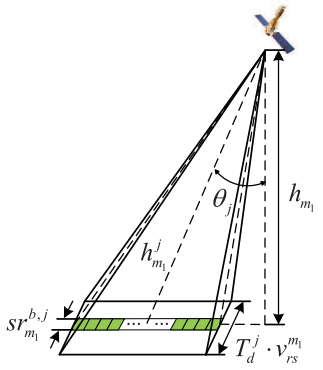

FIGURE 6. Traffic model.

TABLE 4. Imaging task parameter list.

Name	Description	Value
$s^{m_1}_{rs}$	Imaging node for task ri_j	4, 5
T^j_t	Imaging time for task ri_j/s	0, 180
T^j_d	Imaging duration for task ri_j/s	10, 20
θ_j	Imaging swinging degree for task ri_j/°	0, 10
B_{m_1}	Nof bands for $s^{m_1}_{rs}$	11
N^b_p	Nof pixels in line for b-th band	7000
N^b_q	Nof quantization bits for b-th band	12
$sr^b_{m_1}$	Spatial resolution for b-th band in $s^{m_1}_{rs}$/m	10
h_{m_1}	Height of the satellite for $s^{m_1}_{rs}$/Km	700
ρ_b	Data compression rate for b-th band	2

Thus, with the imaging task parameter list showed in Table. 4, the data generated by the given remote sensing satellite $s^{m_1}_{rs}$ can be expressed as

$$F^j_{m_1} = \sum_{b=1}^{B_{m_1}} \left(N^b_p \cdot N^b_q \cdot T^j_d \cdot v^{m_1}_{rs} / (sr^{b,j}_{m_1} \cdot \rho_b)\right) \tag{11}$$

Furthermore, $v^{m_1}_{rs}$ is the speed of satellite $s^{m_1}_{rs}$ on orbit, and can be further expressed as

$$v^{m_1}_{rs} = \sqrt{\mu/(R + h_{m_1})} \tag{12}$$

where μ is the Kepler constant.

Furthermore, the data generated $F^j_{m_1}$ should be quantized by bundle as $Fb^j_{m_1}$, in order to adapt the edge capacity. With the file packaging demonstrated Fig. (5), $Fb^j_{m_1}$ can be expressed as

$$Fb^j_{m_1} = \left\lceil \frac{F^j_{m_1}}{(N_s \cdot (M_s + H_s) + M_r + H_b)} \right\rceil \tag{13}$$

IV. MULTI TASK MINIMUM DELAY ROUTING

A. PROBLEM FORMULATION

Considering of the concurrent bulk data and varying network topology, UDG graph is redesigned with the task data and edge capacity model for delay estimation, combining as TUDG. The Algorithm. (1) introduces the construction procedure of TUDG with mission data model. After initialization, the timestamps in $\mathcal{T}_{tc}$ dominate the algorithm execution. Function *CalData* and *CalCap* are designed according to (13) and (9), respectively. And function *AddVertex* and *AddEdge* can be derive from the basic rules in UDG model.

Algorithm 1 Construction Procedure of UDG With Mission Data Model

INPUT: $\mathcal{S}, \mathcal{GC}, \mathcal{N}, \mathcal{RI}, \mathcal{C}, \mathcal{D}$
OUTPUT: $\mathcal{GU}$
// Record the time instance when topology changes
$\mathcal{T}_{tc} \leftarrow \langle T^k_b, T^k_e, T^j_t + T^j_d | 1 \le k \le K, 1 \le j \le J \rangle$
// Initialization of the serial number of layer and task
$l_u \leftarrow 1, L_u \leftarrow |T_{tc}|, j \leftarrow 1$
// Initialization of the UDG model and current layer time
$\mathcal{GU} \leftarrow \emptyset, t_c \leftarrow T^1_{tc}$
while $l_u \le L_u$ **do**
  $T_f \leftarrow T_c$ *// Updating the former layer time* T_f
  $T_c \leftarrow T^{l_u}_{tc}$ *// Updating the current layer time* T_c
  // Image data acquisition
  if $T_c == T^j_t + T^j_d$ **then**
    $F \leftarrow CalData(\mathcal{S}, ri_j)$ *// Calculate data size*
    $\mathcal{GU} \leftarrow AddEdge(\mathcal{GU}, F, T_c, ri_j, ri_j)$
  end if
  // Check the contacts for in current layer
  for all $k \in \mathcal{C}$ **do**
    if $T_c == T^k_b$ **then**
      // Only updating the contacts in current layer
      $\mathcal{GU} \leftarrow AddVertex(\mathcal{GU}, T_c, n^k_f, n^k_t)$
      $Cap \leftarrow CalCap(\mathcal{N}, \mathcal{D}, \mathcal{C}, T^k_e - T^k_b)$
      $\mathcal{GU} \leftarrow AddEdge(\mathcal{GU}, Cap, T_c, n^k_f, n^k_t)$
    else if $(T_c > T^k_b)\&\&(T_c < T^k_e)$ **then**
      // Updating the contacts in former/current layer
      $\mathcal{GU} \leftarrow AddVertex(\mathcal{GU}, T_c, n^k_f, n^k_t)$
      $Cap_f \leftarrow CalCap(\mathcal{N}, \mathcal{D}, \mathcal{C}, T_c - T_f)$
      $Cap_c \leftarrow CalCap(\mathcal{N}, \mathcal{D}, \mathcal{C}, T^k_e - T_c)$
      $\mathcal{GU} \leftarrow AddEdge(\mathcal{GU}, Cap_f, T_f, n^k_f, n^k_t)$
      $\mathcal{GU} \leftarrow AddEdge(\mathcal{GU}, Cap_c, T_c, n^k_f, n^k_t)$
    end if
  end for
  $l_u \leftarrow l_u + 1$
end while
return $\mathcal{GU}$

Typically, data transmission for task ri_j in RS-DTNet through serial of contacts can be mapped as path set $\mathcal{P}^j_{s,d} = \{P^{j,n_p}_{s,d} | 1 \le n_p \le N_p\}$, from source v_s (e.g. remote sensing satellite) to the destination v_d (e.g. ground center). The path $P^{j,n_p}_{s,d} \in \mathcal{P}^j_{s,d}$ is consisted of vertexes list in TUDG, which can be expressed as $P^{j,n_p}_{s,d} = \langle v_s, \cdots v_u, v_v, \cdots v_d \rangle$. The feasible path is restrained by the edge capacity $Cap^v_u > 0$ between any

adjacent vertexes v_u and v_v. Furthermore, the path capacity $Pc_{s,d}^{n_p}$ is defined as the minimum edge capacity along the corresponding path, expressed as

$$Pc_{s,d}^{n_p} = \min Cap_u^v \quad u, v \in P_{s,d}^{j,n_p} \tag{14}$$

Due to the restricted resource, such as contact capacity and storage onboard, delivery delay is identified as important metric for RS-DTNet, in consideration of the high request on timeliness of remote sensing image data. As mentioned above, the delivery delay D_m for multi remote sensing task $\mathcal{RI}$ is defined as

$$D_m = \max_{1 \le j \le J} D_f^j \tag{15}$$

where D_f^j is the delay for task ri_j, and can be further expressed as

$$D_f^j = \max_{1 \le N_b^j \le N_B^j} D_b^{N_b^j}$$

From (15), in order to minimum the multi-task delivery delay, feasible path should be designed for every bundle, which is difficult to tackle, in consideration of the bulk data for multi tasks in RS-DTNet. Straightforward, image data from ri_j can be distributed to $\mathcal{P}_{s,d}^j$, with $Pd_{s,d}^{n_p}$ indicating data injected in $P_{s,d}^{j,n_p}$, $Pd_{s,d}^{n_p} \le Pc_{s,d}^{n_p}$. The minimum TDD for multi-tasks transmission can be achieved by injection data to path with minimum delivery delay, which can be categorized as path-based routing. However, such minimum delivery delay is related to the $Pd_{s,d}^{n_p}$ on the corresponding path. Path selection for the multi tasks degenerates whenever data is transferred through current 'optimal' path, which challenges the optimal routing design.

Therefore, in this paper, Multi Task Minimum Delay Routing is proposed for the multi tasks, according to flow distribution set $\mathcal{F} = \{\mathcal{F}_j | 1 \le j \le J\}$, where $\mathcal{F}_j = \langle f_{u,v}^j \rangle$ is assigned for task ri_j. Data flow with $f_{u,v}^j$ bundles are dispatched for the edge from v_u to v_v in TUDG, with the capacity constrain. This flow-based routing avoids the path selection procedure, which is dilemmatic to decide $Pd_{s,d}^{n_p}$. The optimal $\mathcal{F}$ with minimum delivery delay for multi tasks can be mapped as an optimization problem, expressed as

$$\text{MinMax } D_m(f_{u,v}^j) \tag{16}$$

$$\text{s.t. } \sum f_{u,w}^j - \sum f_{w,v}^j = 0 \quad 1 \le j \le J \tag{17}$$

$$\sum f_{s,u}^j = \sum f_{v,d}^j = F_j \quad 1 \le j \le J \tag{18}$$

$$0 \le \sum_{j=1}^{J} f_{u,v}^j \le Cap_u^v \tag{19}$$

$$f_{u,v}^j \in \mathbb{N} \tag{20}$$

Such optimization problem is Mixed Integer Programming with constraints. Equation (16) is the optimization objective function, whose variable $f_{u,v}^j$ for every edge in UDG for r_j task. Data flow for individual and multi tasks are confined by flow balance and edge capacity. Equation (17) describes the flow balance for vertexes v_u and v_v. Equation (18) is related with task data model, which indicates the data injected into RS-DTNet. Equation (19) imposes restrictions on the flow, from different task transferred on the same edge. Due to the F_j and Cap_u^v is evaluated by bundle, $f_{u,v}^j$ is defined as nonnegative integer, as demonstrated in Equation (20).

B. ROUTING DESIGN

According to (16 - 20), minimum the multi-task delivery delay can be achieved with reasonable flow distribution. It is notable that, the *Min-Max* problem is difficult to handle, in spite of the linear objective function and constraints. Thus, in this paper, the optimization problem is converted by introducing an extra variable $D^* = \max D_m(f_{u,v}^j), 1 \le j \le J$. Furthermore, due to the data for the multi tasks in RS-DTNet aggregated towards $\mathcal{GC}$, the conceivable edges with more delivery delay is closer to destination. Thus, the optimization objective function (16) can be relaxed to the contacts in $\mathcal{C}_{gs}$. The optimization problem can be rephrased as

$$\text{MinMax } D* \tag{21}$$

$$\text{s.t. } D^* \ge D_m(f_{v,d}^j) \quad 1 \le j \le J \tag{22}$$

$$\sum f_{u,w}^j - \sum f_{w,v}^j = 0 \quad 1 \le j \le J \tag{23}$$

$$\sum f_{s,u}^j = \sum f_{v,d}^j = F_j \quad 1 \le j \le J \tag{24}$$

$$0 \le \sum_{j=1}^{J} f_{u,v}^j \le Cap_u^v \tag{25}$$

$$f_{u,v}^j \in \mathbb{N} \tag{26}$$

Correspondingly, solving the *Min-Max* optimization problem, MTMDR routing strategy $\mathcal{RS}$ is designed, which details the operation for node at given time instance. Typically, $\mathcal{RS}$ is operated with the centralized approach. Algorithm. (2) is proposed with the construction procedure from $\mathcal{F}$ to $\mathcal{RS}$. Function *CalTime* is designed based on the vertex label of UDG, and function *CalDelay* can be regarded as inverse function of (9).

C. COMPLEXITY ANALYSIS

Based on Algorithm. (1) and (2), the routing with minimum multi-task delivery delay can be designed, accompanied by the parameters demonstrated in Table (2 - 3). Correspondingly, the complexity of routing design can be divided into three parts, i.e., construction of TUDG graph, solving of optimization problem and transformation of flow distribution. It can be proven that the complexity of TUDG graph construction and flow distribution transformation are pseudo polynomial. On the other side, with the nonnegative integer constrain on flow in every edge, the optimization problem can be mapped as the 3-Partition Problem [27], which is NP-complete in the strong sense. In order to solve such large scale mixed integer programming, a mathematical programming solver GUROBI is utilized.

Algorithm 2 Routing Strategy Design

INPUT: $\mathcal{GU}, \mathcal{N}, \mathcal{C}$
OUTPUT: $\mathcal{RS}$
// Solve the optimization problem
$\mathcal{F} \leftarrow Solver(\mathcal{GU})$
// Initialization of the routing strategy
$RS \leftarrow \emptyset$, $sn \leftarrow 1$, $n_s, n_d \leftarrow 0$, $T_s, T_d \leftarrow 0$
// Transformation procedure for every $f^j_{u,v} \in \mathcal{F}$
for $1 \le j \le J$ **do**
  for $u \in \mathcal{GU}$ **do**
    for $v \in \mathcal{GU}$ **do**
      if $f^j_{u,v} \neq 0$ **then**
        // Record node of the routing operation
        $n_s \leftarrow u$, $n_d \leftarrow v$
        // Record time of the routing operation
        $T_s \leftarrow CalTime(n_s, \mathcal{N})$
        $T_d \leftarrow T_s + CalDelay(f^j_{u,v}, \mathcal{C})$
        // Record operation in the routing strategy
        $RS(i) \leftarrow \langle sn, n_s, n_d, T_s, T_d, f^j_{u,v} \rangle$
        $sn \leftarrow sn + 1$
      end if
    end for
  end for
end for
return $\mathcal{RS}$

TABLE 5. Simulation parameter list.

Description	Value
Storage on Satellite /Gbite	10
Transmission Rate for ISC /Mbps	50
Bit Error Rate for ISC	10^{-5}
Transmission Rate for GSC /Mbps	100
Bit Error Rate for GSC	10^{-6}
Maximum Sustainable Delay T /s	200
Path Capacity Portion α	0.5
Task Interval Time Δt /s	20

V. PERFORMANCE EVALUATION

A. PARAMETER SETTING

In this section, performance of the proposed Multi Task Minimum Delay Routing is evaluated, compared with the traditional path-based routing strategy, i.e., Earliest Path Routing (EPR) and Random Path Routing (RPR). The basic idea of such path-based routing strategies is finding feasible path for data transmission, without equitable flow distribution. In order to cope with the challenge for concurrent bulk data transmission, Alpha-Earliest Path Routing (AEPR) is proposed as contrast, with detail as

- EPR: Data is transferred to the path with minimum delivery delay, and $Pd^{n_p}_{s,d} = Pc^{n_p}_{s,d}$. Routing is accomplished if all data for RI is scheduled, $\sum_{n^j_p} Pd^{n^j_p}_{s_j,d_j} = F_j$, $1 \le j \le J$.

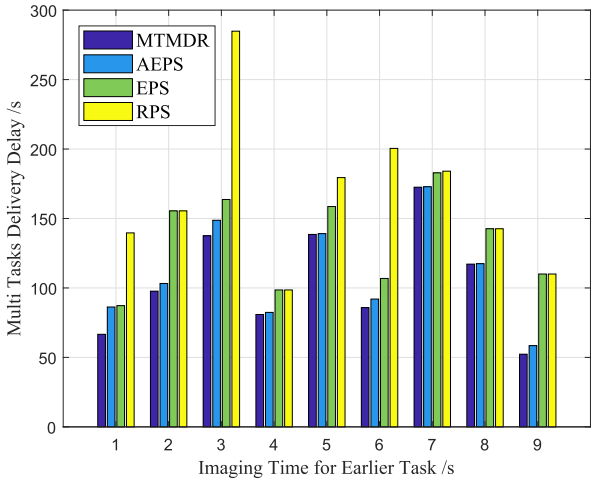

FIGURE 7. Comparison between different routing design with task time interval of 20s.

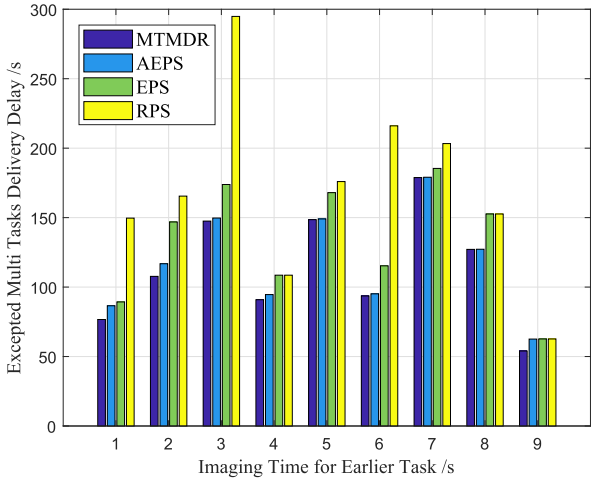

FIGURE 8. Comparison between different routing design with task time interval of 10s.

- RPR: Data is transferred to the random selected path from the source s_j to destination d_j for every $ri_j \in RI$. The condition for routing schedule is similar with EPR.
- AEPR: Similarly, path with minimum delivery delay has higher priority. Path capacity portion parameter α is introduced to indicate the data volume injected, i.e., $Pd^{n_p}_{s,d} = \alpha \cdot Pc^{n_p}_{s,d}$. Thus, data is distributed to more path with equitable distribution.

The simulation environment is based on Matlab, where the contact list is acquired from STK. The representative RS-DTNet simulation scene is built, with 2 remote sensing satellites, 12 data relay satellites and 3 ground center. Specifically, $\mathcal{S}_{rs}$, referred to Landsat, are deployed in sun-synchronous orbit, with altitude of 700 km. The constellation of $\mathcal{S}_{dr}$ is Walker Delta with 4 satellite uniformly distributed in 3 orbits, which is similar to Globalstar. The $\mathcal{GC}$ are placed in Beijing, China, Sioux Falls, South Dakota and Alice Springs, Australia, which is dispersed on

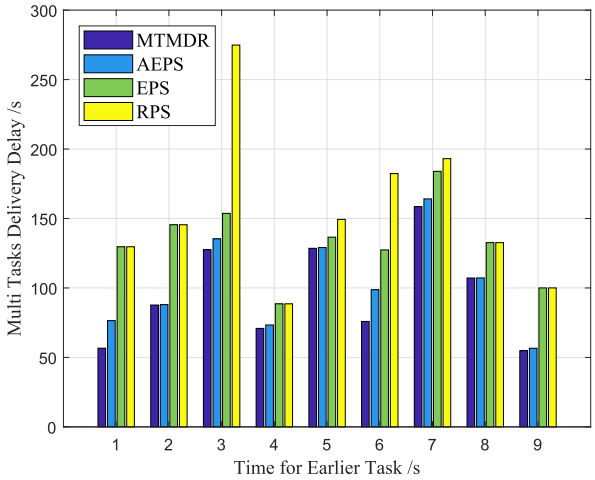

FIGURE 9. Comparison between different routing design with task time interval of 30s.

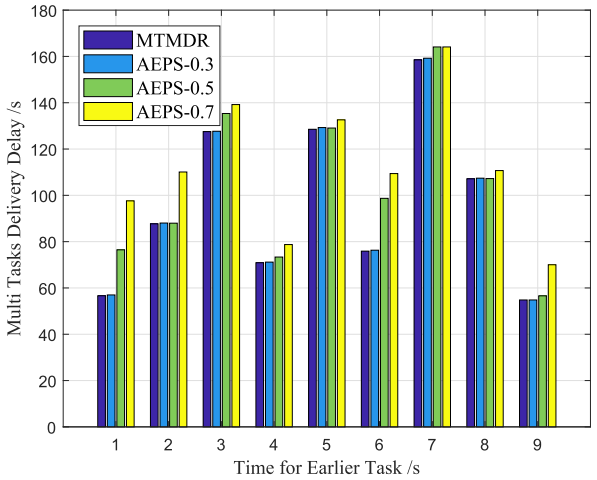

FIGURE 11. Comparison between MTMDR and AEPR with different alpha.

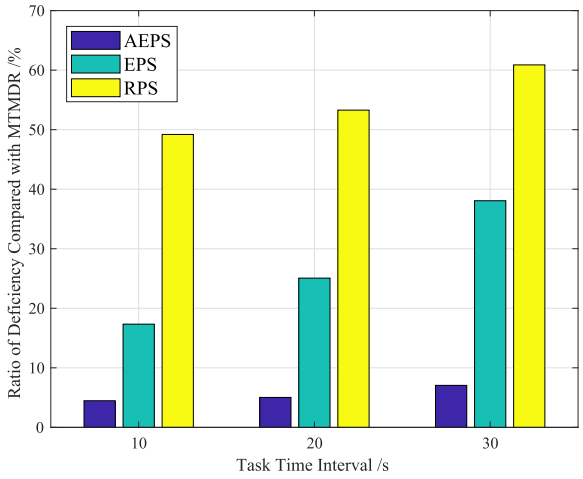

FIGURE 10. Ratio of deficiency compared with MTMDR.

the Earth. Without loss of generality, the parameter of simulation are exhibited in Table. (5). Incorporating with parameters in Table. (4) and (3), the contact list $\mathcal{C}$ is established, and TUDG graph model with data model is designed.

B. SIMULATION RESULTS

For the sake of performance evaluation, delivery delay for multi tasks is taken as metrics. Fig. demonstrates the comparison between different routing design. The imaging time for earlier task varies from 0 to 80000s, with the fixed task interval of 20s. The simulation result verifies the advantage of proposed MTMDR with respect to the delivery delay, benefiting from the rational data distribution. The delivery delay for different routing strategy floats tremendously at different time, affected by the dynamic network topology. Due to purposeless path selection, RPS shows the worst performance.

The impact of task time interval is analyzed, as demonstrated in Fig. (8) - (9) with $\Delta t = 10s$ and $\Delta t = 30s$, respectively. The similar tendency can be drawn, which has a great relationship with the imaging time for earlier task. In order to compare the effect of parameter Δt with further analyses, the ratio of deficiency compared with MTMDR is tested, as shown in Fig. (10). With the increasing of task time interval, the advantages of MTMDR is more obvious.

Furthermore, in order to investigate the data equitable distribution, the performance of MTMDR and AEPR with different α are compared, exhibited in Fig. (11). Intuitively, the value of α is negative related the delivery delay. Especially, the performance of EPS with $\alpha = 0.3$ is slightly worse than MTMDR. Thus, the flow allocation according to MTMDR can be regarded as the optimal condition for AEPR, which is coincident with design principle in (16 - 20).

VI. CONCLUSION

In order to design the routing strategy with minimum delivery delay for bulk and concurrent image data in RS-DTNet, in this paper, multi-task based delivery delay analytical framework is proposed. Based on the TUDG graph with the image data and edge capacity model, the minimum TDD converts as Max-Min optimization problem. In particular, the MTMDR routing is designed, according to the optimal flow distribution deduced from solving such optimization problem. Through the extensively experimental results, the proposed routing algorithm MTMDR shows significant performance improvements with respects to the delivery delay. Furthermore, the flow allocation according to MTMDR can be regarded as the optimal condition for conventional path-based routing.

REFERENCES

[1] W. Yuan and X. Lining, "Remote sensing satellite networking technology and remote sensing system: A survey," presented at the IEEE Int. Conf. Electron. Meas. Instrum., Qingdao, China, Jul. 2015.

[2] S. Peng, H. Chen, C. Du, J. Li, and N. Jing, "Onboard observation task planning for an autonomous earth observation satellite using long short-term memory," *IEEE Access*, vol. 6, pp. 65118–65129, 2018.

[3] H. Cruz-Sánchez, L. Franck, and A.-L. Beylot, "Routing metrics for store and forward satellite constellations," *IET Commun.*, vol. 4, no. 13, pp. 1563–1572, 2010.

[4] Z. Song, G. Dai, M. Wang, and X. Chen, "A novel grid point approach for efficiently solving the constellation-to-ground regional coverage problem," *IEEE Access*, vol. 6, pp. 44445–44458, 2018.

[5] M. J. Khan, H. S. Khan, A. Yousaf, K. Khurshid, and A. Abbas, "Modern trends in hyperspectral image analysis: A review," *IEEE Access*, vol. 6, pp. 14118–14129, 2018.

[6] H. Li and Y. Li, "Optimal path planning for multi-target observation of remote sensing satellite," presented at the IEEE Chin. Guid., Navigat. Control Conf. (CGNCC), Nanjing, China, Aug. 2016.

[7] H. Pucha, Y. Zhang, Z. M. Mao, and Y. C. Hu, "Understanding network delay changes caused by routing events," presented at the ACM SIGMETRICS Int. Conf. Meas. Modeling Comput. Syst., San Diego, CA, USA, Jun. 2007.

[8] *Landsat 8 Data User Handbook—Section 2—Observatory Overview. Geological Survey, Department of the Interior, U.S., Version 3.0.* Accessed: Oct. 2018. [Online]. Available: https://landsat.usgs.gov/landsat-8-l8-data-users-handbook-section-2

[9] J. Storey, D. P. Roy, J. Masek, F. Gascon, J. Dwyer, and M. Choate, "A note on the temporary misregistration of Landsat-8 Operational Land Imager (OLI) and Sentinel-2 Multi Spectral Instrument (MSI) imagery," *Remote Sens. Environ.*, vol. 186, pp. 121–122, Dec. 2016.

[10] Y. Jiang, M. Sun, and C. Yang, "A generic framework for using multi-dimensional Earth observation data in GIS," *Remote Sens.*, vol. 8, no. 2, p. 382, 2016.

[11] R. Radhakrishnan, W. W. Edmonson, F. Afghah, R. M. Rodriguez-Osorio, F. Pinto, and S. C. Burleigh, "Survey of inter-satellite communication for small satellite systems: Physical layer to network layer view," *IEEE Commun. Surveys Tuts.*, vol. 18, no. 4, pp. 2442–2473, 4th Quart., 2016.

[12] S. Gu, J. Jiao, Q. Zhang, and X. Gu, "Rateless coding transmission over multi-state dying erasure channel for SATCOM," *EURASIP J. Wireless Commun. Netw.*, vol. 2017, no. 1, p. 176, Dec. 2017.

[13] Y. Zheng, S. Zhao, Q. Tan, Y. Li, Y. Jiang, and N. Xin, "An analytical framework for remote sensing satellite networks based on the model predictive control with convex optimization," *Int. J. Satell. Commun. Netw.*, vol. 36, no. 3, pp. 305–314, 2018

[14] J. A. Fraire, P. G. Madoery, and J. M. Finochietto, "Traffic-aware contact plan design for disruption-tolerant space sensor networks," *Ad Hoc Netw.*, vol. 47, pp. 41–52, Sep. 2016.

[15] W. Ivancic, W. M. Eddy, D. Stewart, L. Wood, J. Northam, and C. Jackson, "Experience with Delay-Tolerant Networking from orbit," *Int. J. Satell. Commun. Netw.*, vol. 28, pp. 335–351, Sep./Dec. 2010.

[16] X. Sun, Q. Yu, R. Wang, Q. Zhang, Z. Wei, J. Hu, and A. V. Vasilakos, "Performance of DTN protocols in space communications," *Wireless Netw.*, vol. 19, no. 8, pp. 2029–2047, 2013.

[17] R. Wang, A. Sabbagh, S. C. Burleigh, M. Javed, S. Gu, J. Jiao, and Q. Zhang, "Modeling disruption tolerance mechanisms for a heterogeneous 5G network," *IEEE Access*, vol. 6, pp. 25836–25848, 2018.

[18] T. Zhang, H. Li, J. Li, S. Zhang, and H. Shen, "A dynamic combined flow algorithm for the two-commodity max-flow problem over delay-tolerant networks," *IEEE Trans. Wireless Commun.*, vol. 17, no. 23, pp. 7879–7893, Dec. 2018.

[19] Y. Wang, M. Sheng, W. Zhuang, S. Zhang, N. Zhang, R. Liu, and J. Li, "Multi-resource coordinate scheduling for Earth observation in space information networks," *IEEE J. Sel. Areas Commun.*, vol. 36, no. 2, pp. 268–279, Feb. 2018.

[20] P. Yuan *et al.*, "An event-driven graph-based min-cost delivery algorithm in Earth observation DTN networks," presented at the Int. Conf. Wireless Commun. Signal Process., Nanjing, China, Oct. 2015, pp. 15–17.

[21] N. Bezirgiannidis, S. Burleigh, and V. Tsaoussidis, "Delivery time estimation for space bundles," *IEEE Trans. Aerosp. Electron. Syst.*, vol. 49, no. 3, pp. 1897–1910, Jul. 2013.

[22] J. Chen, L. Liu, and X. Hu, "Towards an end-to-end delay analysis of LEO satellite networks for seamless ubiquitous access," *Sci. China Inf. Sci.*, vol. 56, no. 11, pp. 1–13, 2013.

[23] R. Hermenier, C. Kissling, and A. Donner, "A delay model for satellite constellation networks with inter-satellite links," presented at the Int. Workshop Satell. Space Commun., Tuscany, Italy, Sep. 2009, pp. 3–7.

[24] G. Araniti, N. Bezirgiannidis, E. Birrane, I. Bisio, S. Burleigh, C. Caini, M. Feldmann, M. Marchese, J. Segui, and K. Suzuki, "Contact graph routing in DTN space networks: Overview, enhancements and performance," *IEEE Commun. Mag.*, vol. 53, no. 3, pp. 38–46, Mar. 2015.

[25] L. Lei and H. Li, "A routing policy based on time-varying graph for predictable delay tolerant networks," presented at the Int. Conf. Wireless Commun. Signal Process., Nanjing, China, Oct. 2015, pp. 1–6.

[26] R. Wang, Z. Wei, V. Dave, B. Ren, Q. Zhang, J. Hou, and L. Zhou, "Which DTN CLP is best for long-delay cislunar communications with channel-rate asymmetry?" *IEEE Wireless Commun.*, vol. 18, no. 6, pp. 10–16, Dec. 2011.

[27] Q. Liu, L. Deng, H. Zeng, and M. Chen, "On the min-max-delay problem: NP-completeness, algorithm, and integrality gap," presented at the IEEE Inf. Theory Workshop, Kaohsiung, Taiwan, Nov. 2017, pp. 21–25.

[28] P. Yuan, Z. Yang, Q. Zhang, and Y. Wang, "A minimum task-based end-to-end delivery delay routing strategy with updated discrete graph for satellite disruption-tolerant networks," presented at the IEEE/CIC Int. Conf. Commun. China, Beijing, China, Aug. 2018, pp. 293–297.

PENG YUAN received the M.S. degree in communication engineering from the Harbin Institute of Technology (HIT), Shenzhen, China, in 2014, where he is currently pursuing the Ph.D. degree. His current interests include space information networks and disruption-tolerant networks.

ZHIHUA YANG received the Ph.D. degree in communication engineering from the Harbin Institute of Technology (HIT), in 2010. He is currently an Assistant Professor with the Department of Electrical and Information Engineering, HIT's Shenzhen Graduate School, China. His current interests include deep space communications and networking, DTN, and wireless communications.

YE WANG received the M.S. and Ph.D. degrees in information and communication engineering from the Harbin Institute of Technology (HIT), Shenzhen, China, in 2009 and 2013, respectively. From 2013 to 2014, he was a Postdoctoral Research Fellow with the University of Ontario Institute of Technology, Canada. He is currently an Assistant Professor with the HIT. His current research interests include the IoT, edge computing, resource allocation, and the mobile Internet. He received the Best Paper Award of EAI WiSATS 2019, the Outstanding Postdoctoral Award of HIT, Shenzhen Graduate School, in 2016, and the Shenzhen Natural Science Award, in 2017.

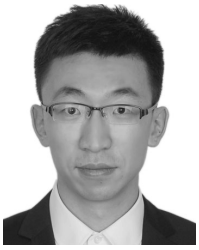

SHUSHI GU received the M.S. and Ph.D. degrees in communication engineering from the Harbin Institute of Technology (HIT), in 2012 and 2016, respectively. Since 2016, he was a Postdoctoral Research Fellow with the Communication Engineering Research Centre, HIT, Shenzhen, China. He is currently a Visiting Scholar and a Research Associate with the NB-IoT Laboratory, James Cook University, Cairns, Australia. He received the Best Paper Awards of IEEE WCSP 2015 and EAI WiSATS 2019. He received the Outstanding Postdoctoral Award of HIT (Shenzhen), in 2018. His current research interests include the satellite IoT, edge caching, distributed storage systems, and distributed coding.

QINYU ZHANG received the bachelor's degree in communication engineering from the Harbin Institute of Technology (HIT), in 1994, and the Ph.D. degree in biomedical and electrical engineering from the University of Tokushima, Japan, in 2003. From 1999 to 2003, he was an Assistant Professor with the University of Tokushima. From 2003 to 2005, he was an Associate Professor with the Shenzhen Graduate School, HIT, where he was also the Founding Director of the Communication Engineering Research Center, School of Electronic and Information Engineering. Since 2005, he has been a Full Professor and the Dean of the EIE School, HIT. His research interests include aerospace communications and networks, wireless communications and networks, cognitive radios, signal processing, and biomedical engineering. He has been a TPC Member of INFOCOM, ICC, GLOBECOM, WCNC, and other flagship conferences in communications. He received three scientific and technological awards from governments and received the National Science Fund for Distinguished Young Scholars, the Young and Middle-Aged Leading Scientist of China, and the Chinese New Century Excellent Talents in University. He was the TPC Co-Chair of the IEEE/CIC ICCC'15, the Symposium Co-Chair of the IEEE VTC'16 Spring, an Associate Chair of Finance of ICMMT'12, and the Symposium Co-Chair of CHINACOM'11. He was the Founding Chair of the IEEE Communications Society Shenzhen Chapter. He is on the Editorial Board of some academic journals, such as the *Journal on Communications*, the *KSII Transactions on Internet and Information Systems*, and *Science China: Information Sciences*.